Langmuir

Article

pubs.acs.org/Langmuir

Myocardial Scaffold-Based Cardiac Tissue Engineering: Application of Coordinated Mechanical and Electrical Stimulations

Bo Wang,[†] Guangjun Wang,[†] Filip To,[†] J. Ryan Butler,[‡] Andrew Claude,[‡] Ronald M. McLaughlin,[‡] Lakiesha N. Williams,[†] Amy L. de Jongh Curry,[§] and Jun Liao*,[†]

[†]Tissue Bioengineering Laboratory, Department of Biological Engineering, and [‡]Department of Clinical Sciences, College of Veterinary Medicine, Mississippi State University, Mississippi State, Mississippi 39762, United States

[§]Department of Biomedical Engineering, University of Memphis, Memphis, Tennessee, 38152, United States

ABSTRACT: Recently, we developed an optimal decellularization protocol to generate 3D porcine myocardial scaffolds, which preserve the natural extracellular matrix structure, mechanical anisotropy, and vasculature templates and also show good cell recellularization and differentiation potential. In this study, a multistimulation bioreactor was built to provide coordinated mechanical and electrical stimulation for facilitating stem cell differentiation and cardiac construct development. The acellular myocardial scaffolds were seeded with mesenchymal stem cells (10^6 cells/mL) by needle injection and subjected to 5-azacytidine treatment (3 μmol/L, 24 h) and various bioreactor conditioning protocols. We found that after 2 days of culturing with mechanical (20% strain) and electrical stimulation (5 V, 1 Hz), high cell density and good cell viability were observed in the reseeded scaffold. Immunofluorescence staining demonstrated that the differentiated cells showed a cardiomyocyte-like phenotype by expressing sarcomeric α-actinin, myosin heavy chain, cardiac troponin T, connexin-43, and *N*-cadherin. Biaxial mechanical testing demonstrated that positive tissue remodeling took place after 2 days of bioreactor conditioning (20% strain + 5 V, 1 Hz); passive mechanical properties of the 2 day and 4 day tissue constructs were comparable to those of the tissue constructs produced by stirring reseeding followed by 2 weeks of static culturing, implying the effectiveness and efficiency of the coordinated simulations in promoting tissue remodeling. In short, the synergistic stimulations might be beneficial not only for the quality of cardiac construct development but also for patients by reducing the waiting time in future clinical scenarios.

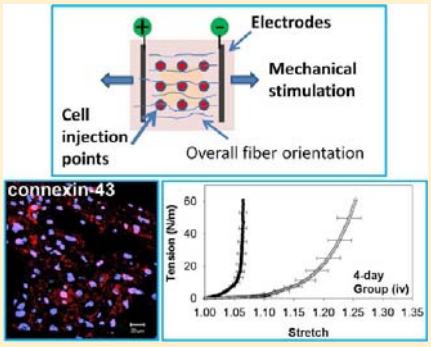

1. INTRODUCTION

Myocardial infarction (MI) and heart failure are the leading causes of mortality globally.[1] When coronary arteries are blocked, the perfusion to the downstream heart muscle is inadequate and can result in cell death.[2] The pathological progression of MI includes inflammatory responses, cardiomyocyte death, scar formation, expansion of infarcted region, and thinning and dilation of the left ventricular (LV) wall.[3,4] Cardiac function deteriorates along with the pathological progression of MI, and in the end stage, arrhythmias, mitral regurgitation, and heart failure can occur and are often fatal.[5,6]

Heart transplantation is an effective treatment for patients with end-stage heart failure but is limited by the shortage of donor hearts.[7] Standard treatments following acute MI involve prompting revascularization with thrombolytic/fibrinolytic therapy, coronary angioplasty, and coronary artery bypass grafting; those treatments are effective in preventing the extension of the infarction but limited in restoring the cardiac function lost as a result of heart muscle death.[8] Recent studies on MI treatment are focused on either avoiding scar formation/triggering tissue remodeling with stem cell injection[9,10] or replacing formed scar tissue with a functioning cardiac construct.[11,12] The hope of these new approaches is not only to prevent further LV dilation and pathological remodeling but also to regenerate myocardial tissues and consequently restore cardiac function. Among the new approaches, cardiac tissue engineering has attracted significant interest in the past three decades because of the great promise of creating viable myocardial tissues.[13−15] Interesting progress has been made in cardiac tissue engineering with contributions from research groups in a variety of disciplinary backgrounds, including stem cells, biomaterials, and tissue-derived scaffolds.[16−18] However, the complexity of myocardium, both structurally and functionally, still presents many challenges for tissue engineering endeavors.

The myocardium is highly organized in structure and possesses unique electrophysiological and mechanical properties.[19] The myocardial fibers have a complex multilayered helical architecture that is essential for well-coordinated heart contraction.[20] Among the individual myocardial fibers is a 3D network of myocardial extracellular matrices (ECM) that are critical to the structural integrity of the myocardium, the tethering of myocytes, the transfer of muscle contractile forces, and the prevention of excessive stretch in muscle fibers.[21−24]

Received: May 5, 2013
Revised: July 9, 2013

   dx.doi.org/10.1021/la401702w | *Langmuir* XXXX, XXX, XXX−XXX

To engineer the contractile and functional equivalent of the native myocardium, the challenges involve not only the generation of high-density functional cardiomyocytes but also the integration of the cells within a 3D ECM/scaffold.[25−27] The mixture of functional cardiomyocytes with ECM/scaffolds needs to reach a delicate balance in order to generate an optimal myocardial construct.[12,28−30] It can be understood logistically that the approaches starting from a high density of cells experience good cell-to-cell connection and capability to propagate electrical propagation but face hurdles in structural strength and mechanical properties.[15,31−33] However, the approaches utilizing polymeric scaffolds and tissue-derived scaffolds often have good mechanical behavior in the construct but encounter challenges in reaching a high reseeding density and cell-to-cell connections and hence lack contractility and electrical transduction.[14,34]

Recently, the potential of acellular myocardial scaffolds has been revealed by Ott et al. in their work on a revitalized beating rat heart made from a decellularized intact rat heart perfused with cardiac and endothelial cells.[35] Early-stage scale-up research on a whole pig heart was also reported and discussed by Badylak et al. and Taylor et al.[36,37] Our group, however, has undertaken an effort to harness the potential of decellularized porcine myocardium as a scaffold material (e.g., for making a cardiac patch).[38,39] Until now, studies have emerged not only on acellular porcine and rat myocardial scaffolds[38−40] but also on acellular human myocardial scaffolds.[41] As shown in our previous publications,[38,39] we have developed an optimal decellularization protocol to generate 3D porcine acellular myocardial scaffolds in which 3D cardiomyocyte lacunae and ECM networks were well preserved along with mechanical anisotropy and vasculature templates;[38,39] the acellular myocardial scaffolds also showed good stem cell recellularization and differentiation potential and experienced positive tissue remodeling manifested by a recovering trend in tissue mechanical properties.[38]

To improve further the effectiveness and efficiency of cell differentiation and tissue remodeling of the stem-cell-reseeded acellular myocardial scaffolds, in this study we have explored the effect of physical stimulations on the outcomes of the tissue construct fabricated with the acellular myocardial scaffolds and mesenchymal stem cells. As pointed out by Vogel et al., physical stimulations can affect the cell proliferation, differentiation, and migration and consequently the biological, mechanical, and other properties of the cardiac construct.[28,42] For cardiac tissue engineering, two types of physical simulations are important in assisting in the development of the tissue construct: one is mechanical stretching, and the other is electrical current stimulation. In an in vitro study, Zhuang et al.[43] reported that 10% cyclic uniaxial stretch produced the upregulation of connexin-43 and *N*-cadherin in the intercellular junctions and increased the propagation velocity. Yamada et al. also reported the cyclic stretch (10%) upregulated expression of both the electrical junction protein (connexin-43) and the mechanical junction proteins (plakoglobin, desmoplakin, and *N*-cadherin) via the integrin-dependent activation of focal adhesion kinase (FAK).[44,45] Moreover, Zimmerman et al.[46] found that the encapsulated neonatal rat cardiomyocytes in a gel matrix formed intensively interconnected, longitudinally oriented cardiac muscle bundles under uniaxial stretching, and the tissue construct showed contractile properties similar to those of native myocardium. For electrical stimulation, Radisic and Vunjak-Novakovic observed that spontaneous construct beating took place in a construct (collagen sponge) reseeded with rat cardiomyocytes under ∼5 V and 1 Hz electrical stimuli.[47,48] In Ott's study,[35] electrical stimulation from a 5−20 V (10 ms) pulse was also applied to the recellularized rat heart using epicardial leads.

The synergistic effects of the mechanical and electrical stimulations on cardiac patch tissue engineering have not yet been fully investigated. We thus designed and fabricated a bioreactor to provide multistimulations to the tissue construct made of the acellular myocardial scaffolds and mesenchymal stem cells (MSCs). We hypothesize that the combined mechanical and electrical stimulations will more efficiently promote cell repopulation, cardiomyocyte differentiation, and remodeling of the engineered cardiac construct. To sort out the effects of the applied mechanical and/or electrical stimulations during in vitro culturing, acellular myocardial scaffolds were reseeded with rat MSCs and subjected to various bioreactor conditioning. The in vitro conditioning parameters examined include mechanical stretching, electrical stimulation, and tissue culture times. The hope is to shed light on how physical stimulation plays a role in the tissue remodeling of the engineered cardiac construct derived from acellular myocardial scaffolds.

2. MATERIALS AND METHODS

2.1. Design of a Multistimulation Bioreactor. The working principle of the multistimulation bioreactor, which was capable of delivering both mechanical and electrical stimulations to the cardiac construct, is shown in Figure 1a,b. Linear movement was applied by a

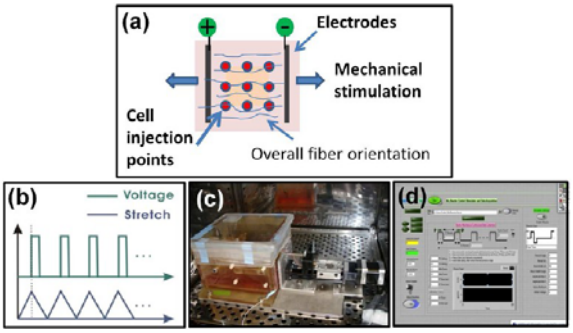

Figure 1. (a) Schematic illustration of the engineered scaffold subjected to cell injection and mechanical and electrical stimulations. (b) Wave forms of the applied mechanical stretch and electrical pulses. (c) Bioreactor placed in the incubator. (d) User interface of the custom-written LabView program.

movable arm driven by an Xslide assembly and a stepper motor (Velmex, New York, NY) (Figure 1c). Electrodes were made from a Teflon-coated silver wire of 75 μm diameter (A-M Systems, Carlsborg, WA). Teflon insulation was stripped from the end of the wire, and the naked wires were inserted into the two opposite edges of the tissue construct. To simulate what myocardial tissue experiences, electrical pulses were applied when each unloading cycle started (Figure 1b). The frequency and amplitude of the cyclic stretches and electrical pulses were controlled by a custom-written LabView program. The program was capable of delivering multiple protocols of mechanical stretching and various waveforms of electrical stimulation (Figure 1d).

The bioreactor chamber and parts were designed using Solidworks 3D CAD software (Solidworks Corp., Concord, MA). The structural elements of the device were machined from either acrylic or polysulfone that provided abrasion resistance and excellent thermal/chemical stability. The bioreactor consisted of one tissue culture chamber, in which two to four pieces of tissue constructs (20 mm × 20

dx.doi.org/10.1021/la401702w | *Langmuir* XXXX, XXX, XXX−XXX

mm × ∼3 mm) could be mounted between a fixed clamp and a movable clamp (Figure 1c). Ti-corn blue sutures (no. 0) were used to connect the sample with two clamps. The cover of the tissue culture chamber was fabricated with $^1/_4$-in.-thick clear polycarbonate (Small Parts, Inc. Logansport, IN). A hole 2 cm in diameter was made on the cover and then sealed with the pentafluoroisopropenyl fluoromethyl ether (PIFE) membrane with 0.2 μm pore size (Millipore, Billerica, MA) to enable air exchange (Figure 1c).

2.2. Preparation of Acellular Myocardial Scaffolds, MSC Reseeding, and Cardiomyocyte Differentiation. *2.2.1. Preparation of Acellular Myocardial Scaffolds.* The decellularization method for porcine myocardium was the same as in our previous study.[39] Forty fresh pig hearts were harvested from ∼6-month-old pigs and transported from the local slaughterhouse to our laboratory in phosphate-buffered saline at 4 °C. From the middle region of the anterior left ventricular wall, we were able to trim square-shaped myocardium samples (20 mm × 20 mm × ∼3 mm), of which one edge aligned along the muscle fiber preferred direction (PD) and the other edge aligned along the cross-fiber preferred direction (XD). Note that the PD direction was determined on the basis of overall muscle fiber texture and heart anatomy.[39] Two edges of the square sample were then perforated with 27G × 31/2 BD Quincke spinal needles that were later affixed by two rectangular plastic frames.[39] The purpose of this frame-pin supporting system was to prevent the contraction of tissue macrogeometry and the collapse of internal cardiomyocytes lacunae.[39] The mounted myocardium samples were then decellularized in a rotating bioreactor using 0.1% sodium dodecyl sulfate (SDS) (Sigma-Aldrich Inc., St. Louis, MO) with 0.01% trypsin (VWR), 1 mM phenylmethylsulfonylfluoride (PMSF, protease inhibitor) (Sigma-Aldrich Inc., St. Louis, MO), 20 μg/mL RNase A (Sigma), 0.2 mg/mL DNase (Sigma-Aldrich Inc., St. Louis, MO), and 100 U/mL penicillin and 100 μg/mL streptomycin at room temperature for 2.5 weeks. Ten-minute ultrasonic treatment (50 Hz, Branson) was applied each day; the solution was changed every 2 days to avoid contamination and tissue deterioration.

2.2.2. MSC Preparation, Reseeding, and Cardiomyocyte Differentiation. Well-characterized Lewis rat mesenchymal stem cells (MSCs, fourth passage) were obtained from the Stem/Progenitor Cell Standardization Core (SPCS) at the Texas A&M Health Science Center (NIH/NCRR grant). These cells were resuspended in mesenchymal stem cell medium (L-DMEM, 10% FBS, 100 U/mL penicillin, and 100 μg/mL streptomycin) and seeded in 175 mm flasks at a density of 3×10^3 cells/cm^2. The medium was changed twice a week. After confluency was reached, aliquots of the MSCs were prepared for reseeding and differentiation.

Before cell reseeding, the square samples of acellular scaffolds were mounted between the fixed clamp and the movable clamp using the surgical Ti-corn blue sutures (no. 0). The acellular scaffolds were then sterilized in 70% ethanol in the tissue culture chamber for 2 h and rinsed with sterilized phosphate-buffered saline (PBS) four times. The entire tissue culture chamber with the mounted scaffolds was further sterilized with UV light for 20 min. After the completion of the sterilization protocol, each scaffold sample was injected with 1 mL of MSC solution at a concentration of 10^6 cells/mL using a syringe (1 mL, 26G Permanent needle, BD Inc.). One milliliter of MSC solution was injected evenly at nine points (∼0.1 mL/point, located in a 3 × 3 array) in the middle region of the square sample (Figure 1a).

After cell injection, the tissue constructs were cultured in 5-azacytidine differentiation medium (L-DMEM, 10% FBS, 3 μmol/L 5-azacytidine (MP Biomedicals Inc.), cardiac myocyte growth supplement (ScienCell Research Laboratories), 100 U/mL penicillin, and 100 μg/mL streptomycin) for the first 24 h. After the 5-azacytidine treatment, the medium was changed to the complete medium (L-DMEM, 10% FBS, cardiac myocyte growth supplement (ScienCell Research Laboratories), 100 U/mL penicillin, and 100 μg/mL streptomycin) for the remaining tissue culture protocols.

2.3. Protocols for in Vitro Bioreactor Conditioning. To compare the influence of mechanical and electrical stimulations on the tissue-engineered cardiac construct, we randomly divided all of the acellular scaffolds into four groups, which were designed as follows: (i) the control group in a static culture; (ii) 20% strain stimulation; (iii) 5 V electrical stimulation; and (iv) 20% strain + 5 V electrical stimulation. For the control group (group i), samples were injected with the same number of MSCs and were placed in the same culture chamber without mechanical or electrical stimulation. For tissue constructs subjected to only stretch conditioning (group ii), samples were mounted between the fixed clamp and the movable clamp and immersed in cell culture medium. For the group given only electrical stimulation (group iii), the positive and negative electrodes were mounted on the two opposite sides of the sample without application of the clamp stretch. For group iv, the stretch and electrical stimulations were simultaneously applied. Note that for the applied stimulations both the triangular strain waveform and square wave electrical pulse were set at a frequency of 1 Hz, which simulates the physiological frequency experienced by the heart muscles. In each group, four tissue constructs were fabricated and used for characterizations such as cell viability, histology, and immunofluorescence staining. For groups subjected to tissue mechanical assessment, four additional tissue constructs were produced and used for biaxial testing.

2.4. Cell Viability, Histology, and Immunohistological Characterizations. *2.4.1. Cell Viability.* Cell viability in the tissue construct was examined with a live/dead assay (L3224, Life Technologies Inc., Grand Island, NY) according to the manufacturer's instructions. Briefly, calcein-AM (2 mM) and ethidium bromide homodimer (4 mM) were mixed in PBS. The tissue constructs were then incubated in the above solution for 20 min at room temperature and rinsed in PBS three times for laser scanning confocal microscopy (LSCM) (Zeiss LSM 510). Ten regions were selected randomly in each sample under high magnification (40×) to analyze the cell viability. The ratio of living cells was estimated by living cells divided by the total number of cells (green indicates living cells and red indicates dead cells).

2.4.2. Histology. Samples prepared for histology were fixed in 2% paraformaldehyde solution for 2 h, embedded in paraffin, subjected to sectioning, stained with hematoxylin and eosin (H&E) or Masson's trichrome, and imaged with bright-field light microscopy (Nikon EC600). Histological images were taken randomly in each section at 40×. The number of reseeded cells was counted in each image, and the cell density was estimated by normalizing the cell number to the area of the selected regions.

2.4.3. Immunofluorescence Staining. For immunofluorescence staining, after rehydration and antigen retrieval with 0.05% trypsin for 10 min at 37 °C, tissue sections were blocked with 1% bovine serum albumin (BSA) for 2 h. Tissue sections were then incubated at 4 °C overnight with primary antibodies targeting myosin heavy chain (GenWay), sarcomeric α-actinin (Sigma), cardiac troponin T (abcam), Connexin-43 (Sigma), or *N*-cadherin (Sigma). After thorough rinsing, secondary antibodies, Cy3 AffiniPure goat antimouse IgG, Cy5 Affini-Pure donkey antimouse IgM, DyLight 649 goat antimouse IgG, and DyLight 549 Affini-Pure donkey anti-mouse IgG (Jackson Immuno Research) were applied at room temperature for 1 h. Finally, all tissue sections were stained with Hoechst (Invitrogen) for cell nuclei. Immunofluorescence slides were observed with an inverted LSCM (Zeiss LSM 510). Positive controls were prepared by following the same protocols with sections of native porcine heart. Negative controls were prepared by following the same protocols with the omission of all of the primary antibodies.

2.5. Biaxial Mechanical Characterization of Tissue Constructs. Biaxial mechanical testing has high sensitivity to capture mechanical behavior changes resulting from subtle structural/compositional alterations in tissues.[38,49,50] Details for biaxial testing such as system setup and testing protocols can be found in the previous publications.[49,50] In this study, biaxial loading was applied along the muscle/scaffold fiber-preferred direction (PD) and cross-preferred direction (XD). After 10-cycle preconditioning, the tissue construct was subjected to an equibiaxial tension protocol (T_{PD}/T_{XD} = 60:60 N/m), where T_{PD} and T_{XD} were the applied tensions along PD and XD, respectively. The extensibility of the tissue construct was characterized by the maximum stretch along PD (λ_{PD}) and the

dx.doi.org/10.1021/la401702w | *Langmuir* XXXX, XXX, XXX−XXX

maximum stretch along XD (λ_{XD}) at an equibiaxial tension of 60 N/m. Tissue constructs were tested in a PBS bath at 37 °C.

2.6. Statistical Analysis. Mean ± standard deviation was used for presenting experimental data. One-way analysis of variance (ANOVA) was applied in statistical analyses, with the Holm-Sidak test for post hoc pairwise comparisons or comparisons versus the control group (SigmaStat 3.0, SPSS Inc., Chicago, IL). The differences were considered to be statistically significant when $p < 0.05$.

3. RESULTS

3.1. Acellular Myocardial Scaffold. An acellular myocardial scaffold was obtained after 2.5 weeks of decellularization treatment. The morphological difference between the acellular myocardial scaffold and the native myocardium is shown in Figure 2a in which the acellular myocardial scaffold

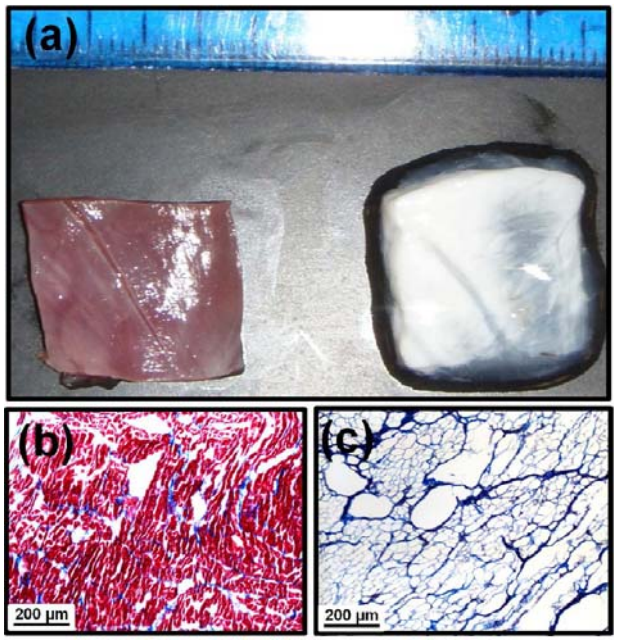

Figure 2. (a) Native (left) and decellularized (right) porcine myocardial scaffold. (b) Mason's trichrome staining of the native porcine myocardium. (c) Mason's trichrome staining of the decellularized myocardial scaffold showing well -preserved cardiomyocyte lacunae. Note that red denotes cardiomyocytes and blue denotes collagen.

exhibits the bright-white color of typical collagenous materials. Complete removal of the cellular contents and good preservation of subtle ECM structure have been verified in our previous publications.[38,39] Cells, cell debris, DNA fragments, and α-Gal porcine antigens were completely removed from the acellular myocardial scaffolds while preserving the myocardial ECM and microstructures such as cardiomyocyte lacunae, blood vessel templates, and cardiac elastin.[38,39] Figure 2b,c shows the histological comparison of the native myocardium and the acellular myocardial scaffold by Mason's trichrome staining.

3.2. Effect of in Vitro Bioreactor Conditioning on Construct Recellularization. The cell density, distribution, and viability after 2 days of tissue culturing were compared among various bioreactor conditioning protocols using H&E and live/dead cell staining (Figure 3). H&E staining showed that the cell densities in the 20% strain stimulation group

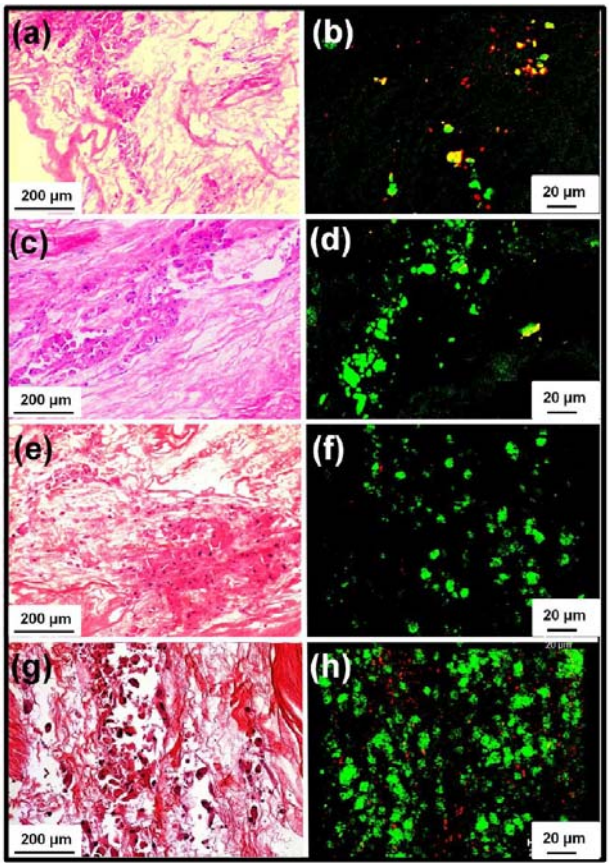

Figure 3. (a) H&E and (b) live/dead staining of the static control group (group i). (c) H&E and (d) live/dead staining of the 20% strain stimulation group (group ii). (e) H&E and (f) live/dead staining of the 5 V electrical stimulation group (group iii). (g) H&E and (h) live/dead staining of the 20% strain + 5 V stimulation group (group iv). Images were taken from the constructs after 2 days of tissue culturing.

(group ii, Figure 3c), 5 V electrical stimulation group (group iii, Figure 3e), and 20% strain + 5 V combined stimulations group (group iv, Figure 3g) are greater than those in the static control group (group i, Figure 3a). Moreover, the live/dead staining results further verified this observation, and the ratios of living cells in the bioreactor conditioning groups (groups ii–iv, Figure 3d,f,h) were also higher than those in the static control group (group i, Figure 3a).

Compared to the static control group (group i, Figure 3a,b), higher cell density and certain cell alignment were observed in the 20% strain stimulation group (group ii, Figure 3c,d); high cell density was also found in the 5 V electrical stimulation group (group (iii, Figure 3e,f), although there were no obvious cell alignments in this group. In the multistimulation group ((20% strain + 5 V, group iv), a higher cell density was observed, and the reseeded cells exhibited better morphology and alignment (Figure 3g,h). Statistical analysis showed that there was a significant difference when comparing group iv to group iii, group ii, or group i ($p < 0.05$, pairwise comparison using the Holm-Sidak method) (Table 1).

It could be seen from the above observation that the multistimulation (20% strain + 5 V, group iv) resulted in better construct recellularization. We further assessed the cell morphologies of the multistimulation group (20% strain + 5 V, group iv) after 1, 2, and 4 days of tissue culturing. Mason's

dx.doi.org/10.1021/la401702w | Langmuir XXXX, XXX, XXX–XXX

Table 1. Cell Density and Ratio of Living Cells of the Static Control Group (Group i), 20% Strain Stimulation Group (Group ii), 5 V Electrical Stimulation Group (Group iii), and 20% Strain + 5 V Stimulation Group (Group iv) after 2 Days of in Vitro Culturing

	group i	group ii	group iii	group iv
reseeded cell density (cells/mm^2)	0.91×10^{2b}	2.21×10^2	2.37×10^2	3.28×10^{2a}
ratio of living cells	51.43%^{b}	80.35%	80.98%	79.38%

^{a}Denotes a significant difference when comparing group iv to group iii, group ii, or group i ($p < 0.05$, pairwise comparison using the Holm-Sidak method). ^{b}Denotes a significant difference when comparing group i to group ii, group iii, or group iv ($p < 0.05$, pairwise comparison using the Holm-Sidak method).

trichrome staining showed that after 2 day of the combined stimulations the cells showed good morphology of cell aggregation (Figure 4b); this trend was even more obvious in the 4 day combined stimulation group (Figure 4c).

3.3. Cell Phenotype Characterizations. As shown in section 3.2, we found that the combination of 20% strain and 5 V electrical stimulation (group iv) generated the best result when compared to other conditioning protocols. The tissue constructs subjected to 20% + 5 V combined stimulations were thus processed for cell phenotype characterization using immunofluorescence staining. Figure 5 showed that the differentiated cells displayed a cardiomyocyte-like phenotype by expressing myosin heavy chain, sarcomeric α-actinin, and cardiac troponin T (Figure 5a–c). The existence of an electrical gap junction protein and an adherens junction protein was also verified by positive staining of connexin-43 and *N*-cadherin, respectively (Figure 5d,e). There was no positive staining in the negative controls, which indicates that the immunohistological images (Figure 5) showed specific staining.

3.4. Biaxial Mechanical Properties. The biaxial tissue behavior of the native myocardium, decellularized myocardial scaffolds, 2 and 4 day static control groups (group i), and 2 and 4 day combined stimulation groups (20% strain + 5 V, group iv) was evaluated, and the averaged stress–strain curves are plotted in Figure 6. The tissue extensibilities were compared by the maximum stretches in the PD direction and the XD direction (Table 2). Both the PD and XD directions of the decellularized myocardium scaffold showed stiffer stress–strain responses ($p < 0.01$) (Figure 6b compared to Figure 6a). By examining the stress–strain curves in Figure 6, we found that panel f (i.e., 4 days of in vitro conditioning with 20% strain and 5 V electrical simulations) showed nonlinear anisotropic mechanical behavior that was close to the biaxial behavior of the native myocardium (Figure 6f compared to Figure 6a). This recovery trend in biomechanical behavior was more evident when comparing the native myocardium (Figure 6a), acellular myocardial scaffolds (Figure 6b), 2 days of multistimulation conditioning (Figure 6e), and 4 days of multistimulation conditioning (Figure 6f). The 2 and 4 day static control groups (Figure 6c,d) showed a small softening trend when compared to the acellular myocardial scaffolds (Figure 6b), which can be explained by the remodeling of the injected cells. However, we noticed that the tissue constructs of the static control group (Figure 6c,d) exhibited less anisotropy when compared to the multistimulation group (Figure 6e,f).

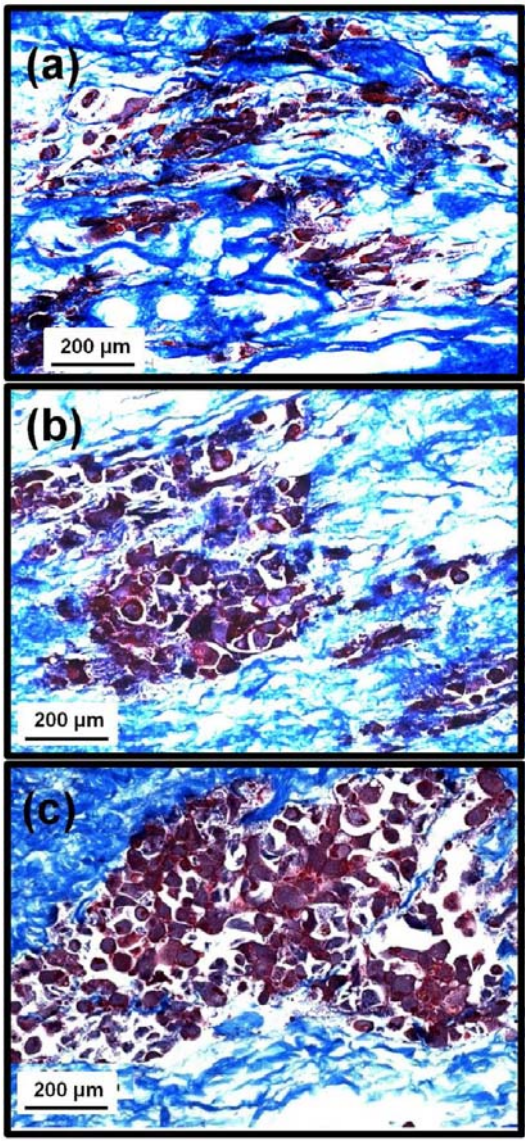

Figure 4. Mason's trichrome staining of tissue constructs of group iv (a) after 1 day of bioreactor conditioning, (b) after 2 days of bioreactor conditioning, and (c) after 4 days of bioreactor conditioning. Group iv delivers 20% strain + 5 V stimulations.

4. DISCUSSION

In our previous studies, the rotating bioreactor[38] allowed better oxygenation of the recellularized scaffolds than did static tissue culturing; however, the efficiency of recellularization and cell differentiation were still relatively low. In this project, the multistimulation bioreactor has been designed and built to provide mechanical stretch to the tissue construct periodically and to apply electrical pulses to stimulate cell differentiation and construct development. During the study, the bioreactor was able to ensure good cell viability under sterile conditions for an extended period of time, and experiments showed excellent reproducibility. Other advantages of the designed multistimulation bioreactor are easy sample mounting, visibility of the sample chamber, and flexibility in implementing complicated protocols.

dx.doi.org/10.1021/la401702w | *Langmuir* XXXX, XXX, XXX–XXX

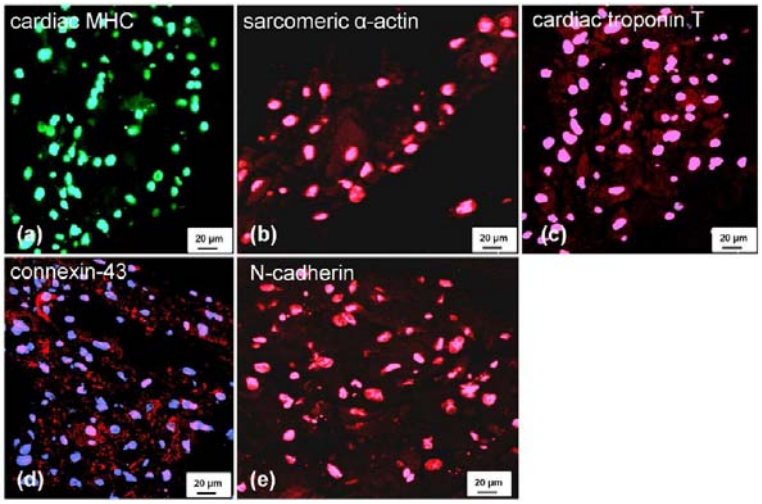

Figure 5. Immunofluorescence staining of tissue constructs after 2 days of bioreactor conditioning (group iv: 20% strain + 5 V). The reseeded cells exhibited a cardiomyocyte-like phenotype by expressing (a) myosin heavy chain (MHC), (b) sarcomeric *α*-actinin, and (c) troponin T; the electrical gap junction protein and adherens junction protein were verified by (d) connexin-43 and (e) *N*-cadherin staining.

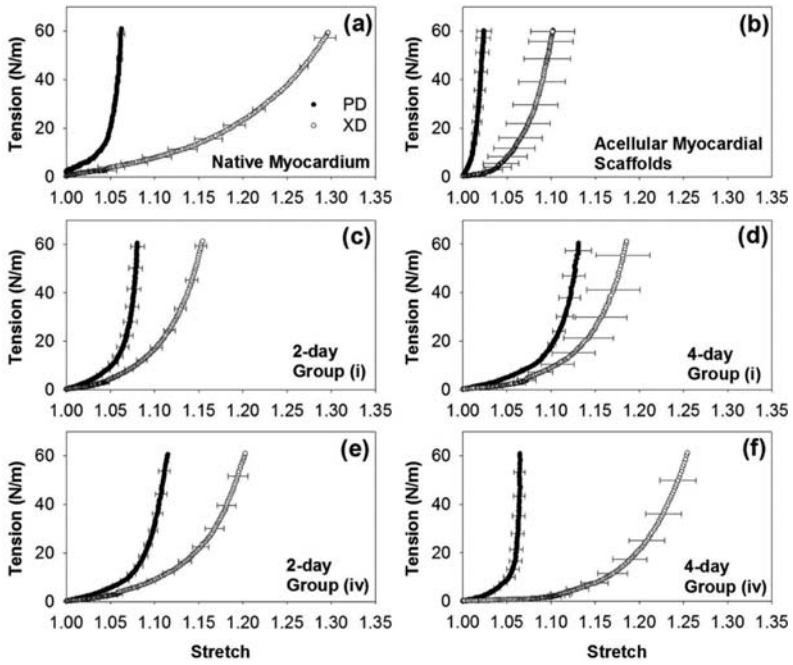

Figure 6. Biaxial mechanical behavior: (a) native myocardium, (b) acellular myocardial scaffolds, (c) 2 day static control (group i), (d) 4 day static control (group i), (e) 2 day in vitro conditioning (group iv: 20% strain + 5 V), and (f) 4 day in vitro conditioning (group iv: 20% strain + 5 V).

Table 2. Biaxial Mechanical Properties of the Native Myocardium, Acellular Myocardial Scaffolds, and Tissue Constructs of Groups i and iv after 2 and 4 Days of Culturing

			group i		group iv	
	native	acellular	2 days	4 days	2 days	4 days
maximum stretch (PD)	1.062 ± 0.004	1.024 ± 0.008[a]	1.080 ± 0.008	1.131 ± 0.015[a]	1.115 ± 0.007	1.065 ± 0.006
maximum stretch (XD)	1.293 ± 0.012	1.102 ± 0.025[a]	1.154 ± 0.006[a]	1.186 ± 0.030[a]	1.203 ± 0.012[a]	1.254 ± 0.021

[a]Denotes a significant difference when compared to the native myocardium ($p < 0.05$).

To increase the efficiency of cell reseeding, we employed a needle injection method for cell implanting with a total cell quantity of 10^6 cells/scaffold in this study. The scaffold was injected at nine points (~0.1 mL/point) that were separated evenly within the central square region (~1 cm × 1 cm). During the injection, effort was taken to ensure that the implanted cells were distributed in an even manner. However, because of the porous structure of the acellular myocardial

dx.doi.org/10.1021/la401702w | *Langmuir* XXXX, XXX, XXX−XXX

scaffold, a small amount of leakage did happen during cell injection. For this kind of situation, we injected the leaked medium back into the same region of the acellular patch.

To explore further the effects of mechanical stimulation alone, electrical stimulation alone, and the combined mechanical and electrical stimulations on cell repopulation and alignment, we compared the cell density, morphology, and viability after 2 days of in vitro culturing among the static control (group i), 20% strain stimulation (group ii), 5 V electrical stimulation (group iii), and 20% strain + 5 V combined stimulations (group iv). The cell density of the control group after 2 days of culturing was 0.91×10^2 cells/mm^2, and no obvious cell alignment was found (Figure 3a). In the bioreactor conditioning groups, the cell densities were 2.21×10^2 cells/mm^2 (group ii), 2.37×10^2 cells/mm^2 (group iii), and 3.28×10^2 cells/mm^2 (group iv). Using the Holm-Sidak method for pairwise multiple comparison, we found that there was a significant difference when comparing group iv to group iii or group ii ($p < 0.05$), which demonstrated that the combined mechanical and electrical stimulations (group iv) promoted cell repopulation in the myocardial scaffolds (Figure 3c,e,g, Table 1). Although there was no obvious cell alignment in group iii (Figure 3e,f), cell alignment was observed in both groups ii and iv (Figure 3c,d,g,h), implicating that the mechanical stimulation likely assisted in cell alignment during in vitro conditioning.

Previous studies have shown that cyclic mechanical stimulation can assist with cell alignment, stimulate ECM formation,[51,52] and improve the cardiomyocytes' development and function.[46,53] Our findings are consistent with the observations of the above-mentioned studies focusing on mechanical stimulation.[46,51−53] Because the cell density of the combined stimulations (20% strain + 5 V, group iv) (Figure 3g) was higher than the 20% strain stimulation (group ii) (Figure 3c), it might indicate that electrical stimulation, along with mechanical stimulation, seems to have a synergistic effect. Electrical stimulation is believed to be able to induce transient calcium levels that will in turn further improve the quantity and organization of sarcomeres in the cardiac tissue.[54] Furthermore, electrical stimulation has been found to facilitate cell proliferation and promote the formation and localization of electric gap junctions.[55,56] Our results show that synergistic treatment with both mechanical and electrical simulations did promote the repopulation and alignment of the reseeded cells.

Biaxial testing results further show that the 20% strain + 5 V stimulations (group iv) generated a good tissue remodeling trend (Figure 6e,f) and desirable nonlinear anisotropic tissue construct behavior (Figure 6f) (i.e., 4 day in vitro conditioning of group iv resulted in a biaxial stress−strain behavior (Figure 6f, Table 2) similar to that of the native myocardium (Figure 6a, Table 2)). Our observations of recellularization and tissue mechanical behavior demonstrate positive tissue remodeling taking place in group iv (20% strain + 5 V) (Figure 6, Table 2).

To understand further the synergistic effects of multi-stimulation on stem cell differentiation, we performed immunofluorescence staining on the tissue constructs produced by 2 days of multisimulations (20% strain + 5 V, group iv). Our results indicated that the differentiated cells clearly demonstrated cardiomyocyte-like phenotypes by abundantly expressing myosin heavy chain, sarcomeric α-actinin, and cardiac troponin T (Figure 5a−c). Connexin-43 and *N*-cadherin were also observed in tissue constructs (Figure 5d,e). As we know, connexin-43 is the major electrical gap junction protein, and *N*-cadherin is the fascia adherens junction protein in heart muscles. These junction proteins play important roles in synchronizing and coordinating the myocardium contraction.[57,58] The myocardium contracts synchronously because ion currents are conducted through the tissue by intercellular gap junctions, which directly couple the cytoplasmic compartments of adjacent cells.[57,58] Yamada et al. found that mechanical stretch could upregulate the expression of both electrical and mechanical junction proteins.[44] Zhuang et al. also proved that an in vitro pulsatile linear stretch could upregulate the expression of both electrical and mechanical junction proteins.[43] Our study also demonstrated that the combined mechanical and electrical stimulations facilitated the formation of electrical gap junctions and mechanical junctions.

5. CONCLUSIONS

In this study, we have successfully built a bioreactor that is able to apply both mechanical and electrical stimulations to facilitate tissue construct development. We found that the recellularization, cardiomyocyte differentiation, and tissue remodeling were more effectively and efficiently promoted by the combined mechanical and electrical stimulations (20% strain + 5 V, group iv). The benefit of this combination of stimulations (20% strain + 5 V) was evidenced by good cell viability, repopulation, differentiation, and positive tissue remodeling within a short period of time (2−4 days). In future clinical settings, patients will have to wait for cell expansion, tissue culturing, and cell reconstruction until a regenerated functional tissue can be applied in surgical treatment. Our results show that the synergistic stimulations might be beneficial not only for the quality of cardiac construct development but also for patients by reducing the waiting time in future clinical scenarios.

6. LIMITATIONS AND FUTURE STUDIES

Because of the structural complexity of the bioreactor, we adopted 70% ethanol sterilization for the acellular myocardial scaffolds and the culturing chamber; for the other parts of the bioreactor that could not be immersed in ethanol, we used UV light for sterilization. The sterilization protocol can be further optimized to reduce sterilizing treatments to a minimal level. As for mechanical stretch, the applied tissue construct strain was estimated by normalizing the displacement of the movable arm to the original distance of two sample mounting arms. The use of the clamp-to-clamp displacement in strain estimation was not an ideal method of accurately measuring the tissue construct strain. Our future improvement will be the real-time tracking of markers on the tissue construct using a camera.

In the bioreactor conditioning protocols, note that only simple combinations were examined in this study because of an excessive workload. More complicated combination of stimulations will be investigated in the future because changes in parameters in mechanical and electrical simulation (e.g., various stretch levels, voltage magnitudes, stimulation frequencies) will likely affect the structural alignment, cell−scaffold interaction, and construct remodeling accordingly. Moreover, we have not observed the electrophysiological response in the engineered cardiac tissue constructs using a microelectrode array technique developed for in vitro measurement.[59] The lack of electrophysiological response is likely caused by the still low cell density (compared with native tissue) and lack of cell-to-cell connections both locally and globally in our current tissue constructs. In short, future investigation is warranted to identify

dx.doi.org/10.1021/la401702w | *Langmuir* XXXX, XXX, XXX−XXX

the optimal reseeding and bioreactor conditioning protocols in order to produce functional cardiac tissue. Finally, a future study will assess the potential of the engineered construct in cardiac repair/regeneration using a well-established rat model.[60]

AUTHOR INFORMATION

Corresponding Author

*Tel: 662-325-5987. Fax: 662-325-3853. E-mail: jliao@abe.msstate.edu.

Notes

The authors declare no competing financial interest.

ACKNOWLEDGMENTS

This study is supported by NIH National Heart, Lung, and Blood Institute grant HL097321. We also would like to acknowledge the support from American Heart Association (13GRNT17150041) and MAFES Strategic Research Initiative (CRESS MIS-361020).

REFERENCES

(1) Roger, V. L.; Go, A. S.; Lloyd-Jones, D. M.; Benjamin, E. J.; Berry, J. D.; Borden, W. B.; Bravata, D. M.; Dai, S.; Ford, E. S.; Fox, C. S.; Fullerton, H. J.; Gillespie, C.; Hailpern, S. M.; Heit, J. A.; Howard, V. J.; Kissela, B. M.; Kittner, S. J.; Lackland, D. T.; Lichtman, J. H.; Lisabeth, L. D.; Makuc, D. M.; Marcus, G. M.; Marelli, A.; Matchar, D. B.; Moy, C. S.; Mozaffarian, D.; Mussolino, M. E.; Nichol, G.; Paynter, N. P.; Soliman, E. Z.; Sorlie, P. D.; Sotoodehnia, N.; Turan, T. N.; Virani, S. S.; Wong, N. D.; Woo, D.; Turner, M. B. Heart disease and stroke statistics–2012 update: a report from the American Heart Association. *Circulation* **2012**, *125*, e2−e220.

(2) Raab, W. The nonvascular metabolic myocardial vulnerability factor in "coronary heart disease". Fundamentals of pathogenesis, treatment, and prevention. *Am. Heart J.* **1963**, *66*, 685−706.

(3) Baroldi, G. Coronary heart disease: significance of the morphologic lesions. *Am. Heart J.* **1973**, *85*, 1−5.

(4) Narula, J.; Haider, N.; Virmani, R.; DiSalvo, T. G.; Kolodgie, F. D.; Hajjar, R. J.; Schmidt, U.; Semigran, M. J.; Dec, G. W.; Khaw, B. A. Apoptosis in myocytes in end-stage heart failure. *N. Engl. J. Med.* **1996**, *335*, 1182−1189.

(5) Cleutjens, J. P.; Blankesteijn, W. M.; Daemen, M. J.; Smits, J. F. The infarcted myocardium: simply dead tissue, or a lively target for therapeutic interventions. *Cardiovasc. Res.* **1999**, *44*, 232−241.

(6) De Celle, T.; Cleutjens, J. P.; Blankesteijn, W. M.; Debets, J. J.; Smits, J. F.; Janssen, B. J. Long-term structural and functional consequences of cardiac ischaemia-reperfusion injury in vivo in mice. *Exp. Physiol.* **2004**, *89*, 605−165.

(7) Cooper, D. K. Donor heart resuscitation and storage. *Surg. Gynecol. Obstet.* **1975**, *140*, 621−31.

(8) Topol, E. J. Current status and future prospects for acute myocardial infarction therapy. *Circulation* **2003**, *108*, III6−III13.

(9) Laflamme, M. A.; Zbinden, S.; Epstein, S. E.; Murry, C. E. Cell-based therapy for myocardial ischemia and infarction: pathophysiological mechanisms. *Annu. Rev. Pathol.* **2007**, *2*, 307−339.

(10) Sharma, R.; Raghubir, R. Stem cell therapy: a hope for dying hearts. *Stem Cells Dev.* **2007**, *16*, 517−536.

(11) Fujimoto, K. L.; Tobita, K.; Merryman, W. D.; Guan, J.; Momoi, N.; Stolz, D. B.; Sacks, M. S.; Keller, B. B.; Wagner, W. R. An elastic, biodegradable cardiac patch induces contractile smooth muscle and improves cardiac remodeling and function in subacute myocardial infarction. *J. Am. Coll. Cardiol.* **2007**, *49*, 2292−2300.

(12) Leor, J.; Aboulafia-Etzion, S.; Dar, A.; Shapiro, L.; Barbash, I. M.; Battler, A.; Granot, Y.; Cohen, S. Bioengineered cardiac grafts: A new approach to repair the infarcted myocardium? *Circulation* **2000**, *102*, III56−III61.

(13) Langer, R.; Vacanti, J. P. Tissue engineering. *Science* **1993**, *260*, 920−926.

(14) Zimmermann, W. H.; Melnychenko, I.; Eschenhagen, T. Engineered heart tissue for regeneration of diseased hearts. *Biomaterials* **2004**, *25*, 1639−1647.

(15) Bursac, N.; Papadaki, M.; Cohen, R. J.; Schoen, F. J.; Eisenberg, S. R.; Carrier, R.; Vunjak-Novakovic, G.; Freed, L. E. Cardiac muscle tissue engineering: toward an in vitro model for electrophysiological studies. *Am. J. Physiol.* **1999**, *277*, H433−H444.

(16) Orlic, D.; Hill, J. M.; Arai, A. E. Stem cells for myocardial regeneration. *Circ. Res.* **2002**, *91*, 1092−1102.

(17) Giraud, M. N.; Armbruster, C.; Carrel, T.; Tevaearai, H. T. Current state of the art in myocardial tissue engineering. *Tissue Eng* **2007**, *13*, 1825−1836.

(18) Akhyari, P.; Kamiya, H.; Haverich, A.; Karck, M.; Lichtenberg, A. Myocardial tissue engineering: the extracellular matrix. *Eur. J. Cardiothorac. Surg.* **2008**, *34*, 229−241.

(19) Zimmermann, W. H.; Didie, M.; Doker, S.; Melnychenko, I.; Naito, H.; Rogge, C.; Tiburcy, M.; Eschenhagen, T. Heart muscle engineering: an update on cardiac muscle replacement therapy. *Cardiovasc. Res.* **2006**, *71*, 419−429.

(20) Zhang, S.; Crow, J. A.; Yang, X.; Chen, J.; Borazjani, A.; Mullins, K. B.; Chen, W.; Cooper, R. C.; McLaughlin, R. M.; Liao, J. The correlation of 3D DT-MRI fiber disruption with structural and mechanical degeneration in porcine myocardium. *Ann. Biomed. Eng.* **2010**, *38*, 3084−3095.

(21) Walker, C. A.; Spinale, F. G. The structure and function of the cardiac myocyte: a review of fundamental concepts. *J. Thorac. Cardiovasc. Surg.* **1999**, *118*, 375−382.

(22) Weber, K. T. Cardiac interstitium in health and disease: the fibrillar collagen network. *J. Am. Coll. Cardiol.* **1989**, *13*, 1637−1652.

(23) Holmes, J. W.; Borg, T. K.; Covell, J. W. Structure and mechanics of healing myocardial infarcts. *Annu. Rev. Biomed. Eng.* **2005**, *7*, 223−253.

(24) Humphery, J. D. *Cardiovascular Solid Mechanics: Cells, Tissues, and Organs*; Springer: New York, 2002.

(25) Wall, S. T.; Walker, J. C.; Healy, K. E.; Ratcliffe, M. B.; Guccione, J. M. Theoretical impact of the injection of material into the myocardium: a finite element model simulation. *Circulation* **2006**, *114*, 2627−2635.

(26) Chen, Q. Z.; Bismarck, A.; Hansen, U.; Junaid, S.; Tran, M. Q.; Harding, S. E.; Ali, N. N.; Boccaccini, A. R. Characterisation of a soft elastomer poly(glycerol sebacate) designed to match the mechanical properties of myocardial tissue. *Biomaterials* **2008**, *29*, 47−57.

(27) Simpson, D.; Liu, H.; Fan, T. H.; Nerem, R.; Dudley, S. C., Jr. A tissue engineering approach to progenitor cell delivery results in significant cell engraftment and improved myocardial remodeling. *Stem Cells* **2007**, *25*, 2350−2357.

(28) Radisic, M.; Park, H.; Gerecht, S.; Cannizzaro, C.; Langer, R.; Vunjak-Novakovic, G. Biomimetic approach to cardiac tissue engineering. *Philos. Trans. R. Soc. London, Part B* **2007**, *362*, 1357−1368.

(29) Kellar, R. S.; Shepherd, B. R.; Larson, D. F.; Naughton, G. K.; Williams, S. K. Cardiac patch constructed from human fibroblasts attenuates reduction in cardiac function after acute infarct. *Tissue Eng* **2005**, *11*, 1678−1687.

(30) Schachinger, V.; Assmus, B.; Britten, M. B.; Honold, J.; Lehmann, R.; Teupe, C.; Abolmaali, N. D.; Vogl, T. J.; Hofmann, W. K.; Martin, H.; Dimmeler, S.; Zeiher, A. M. Transplantation of progenitor cells and regeneration enhancement in acute myocardial infarction: final one-year results of the TOPCARE-AMI Trial. *J. Am. Coll. Cardiol.* **2004**, *44*, 1690−1699.

(31) McSpadden, L. C.; Kirkton, R. D.; Bursac, N. Electrotonic loading of anisotropic cardiac monolayers by unexcitable cells depends on connexin type and expression level. *Am. J. Physiol.: Cell Physiol.* **2009**, *297*, C339−C351.

(32) Bian, W.; Liau, B.; Badie, N.; Bursac, N. Mesoscopic hydrogel molding to control the 3D geometry of bioartificial muscle tissues. *Nat. Protoc.* **2009**, *4*, 1522−1534.

(33) Bursac, N.; Loo, Y.; Leong, K.; Tung, L. Novel anisotropic engineered cardiac tissues: studies of electrical propagation. *Biochem. Biophys. Res. Commun.* **2007**, *361*, 847−853.
(34) Zimmermann, W. H.; Eschenhagen, T. Cardiac tissue engineering for replacement therapy. *Heart Failure Rev.* **2003**, *8*, 259−269.
(35) Ott, H. C.; Matthiesen, T. S.; Goh, S. K.; Black, L. D.; Kren, S. M.; Netoff, T. I.; Taylor, D. A. Perfusion-decellularized matrix: using nature's platform to engineer a bioartificial heart. *Nat. Med.* **2008**, *14*, 213−221.
(36) Badylak, S. F.; Taylor, D.; Uygun, K. Whole-organ tissue engineering: decellularization and recellularization of three-dimensional matrix scaffolds. *Annu. Rev. Biomed. Eng.* **2011**, *13*, 27−53.
(37) Wainwright, J. M.; Czajka, C. A.; Patel, U. B.; Freytes, D. O.; Tobita, K.; Gilbert, T. W.; Badylak, S. F. Preparation of cardiac extracellular matrix from an intact porcine heart. *Tissue Eng., Part C* **2010**, *16*, 525−532.
(38) Wang, B.; Borazjani, A.; Tahai, M.; Curry, A. L.; Simionescu, D. T.; Guan, J.; To, F.; Elder, S. H.; Liao, J. Fabrication of cardiac patch with decellularized porcine myocardial scaffold and bone marrow mononuclear cells. *J. Biomed. Mater. Res. A* **2010**, *94*, 1100−1110.
(39) Wang, B.; Tedder, M. E.; Perez, C. E.; Wang, G.; de Jongh Curry, A. L.; To, F.; Elder, S. H.; Williams, L. N.; Simionescu, D. T.; Liao, J. Structural and biomechanical characterizations of porcine myocardial extracellular matrix. *J. Mater. Sci. Mater. Med.* **2012**, *23*, 1835−1847.
(40) Taylor, D. A.; Atkins, B. Z.; Hungspreugs, P.; Jones, T. R.; Reedy, M. C.; Hutcheson, K. A.; Glower, D. D.; Kraus, W. E. Regenerating functional myocardium: improved performance after skeletal myoblast transplantation. *Nat. Med.* **1998**, *4*, 929−933.
(41) Godier-Furnemont, A. F.; Martens, T. P.; Koeckert, M. S.; Wan, L.; Parks, J.; Arai, K.; Zhang, G.; Hudson, B.; Homma, S.; Vunjak-Novakovic, G. Composite scaffold provides a cell delivery platform for cardiovascular repair. *Proc. Natl. Acad. Sci. U.S.A.* **2011**, *108*, 7974−9.
(42) Vogel, V.; Sheetz, M. Local force and geometry sensing regulate cell functions. *Nat. Rev. Mol. Cell. Biol.* **2006**, *7*, 265−275.
(43) Zhuang, J.; Yamada, K. A.; Saffitz, J. E.; Kleber, A. G. Pulsatile stretch remodels cell-to-cell communication in cultured myocytes. *Circ. Res.* **2000**, *87*, 316−322.
(44) Yamada, K.; Green, K. G.; Samarel, A. M.; Saffitz, J. E. Distinct pathways regulate expression of cardiac electrical and mechanical junction proteins in response to stretch. *Circ. Res.* **2005**, *97*, 346−353.
(45) Shanker, A. J.; Yamada, K.; Green, K. G.; Yamada, K. A.; Saffitz, J. E. Matrix-protein-specific regulation of Cx43 expression in cardiac myocytes subjected to mechanical load. *Circ. Res.* **2005**, *96*, 558−566.
(46) Zimmermann, W. H.; Melnychenko, I.; Wasmeier, G.; Didie, M.; Naito, H.; Nixdorff, U.; Hess, A.; Budinsky, L.; Brune, K.; Michaelis, B.; Dhein, S.; Schwoerer, A.; Ehmke, H.; Eschenhagen, T. Engineered heart tissue grafts improve systolic and diastolic function in infarcted rat hearts. *Nat. Med.* **2006**, *12*, 452−458.
(47) Radisic, M.; Euloth, M.; Yang, L.; Langer, R.; Freed, L. E.; Vunjak-Novakovic, G. High-density seeding of myocyte cells for cardiac tissue engineering. *Biotechnol. Bioeng.* **2003**, *82*, 403−414.
(48) Radisic, M.; Yang, L.; Boublik, J.; Cohen, R. J.; Langer, R.; Freed, L. E.; Vunjak-Novakovic, G. Medium perfusion enables engineering of compact and contractile cardiac tissue. *Am. J. Physiol. Heart Circ. Physiol.* **2004**, *286*, H507−H516.
(49) Grashow, J. S.; Yoganathan, A. P.; Sacks, M. S. Biaixal stress-stretch behavior of the mitral valve anterior leaflet at physiologic strain rates. *Ann. Biomed. Eng.* **2006**, *34*, 315−325.
(50) Liao, J.; Joyce, E. M.; Sacks, M. S. Effects of decellularization on the mechanical and structural properties of the porcine aortic valve leaflet. *Biomaterials* **2008**, *29*, 1065−1074.
(51) Rubbens, M. P.; Driessen-Mol, A.; Boerboom, R. A.; Koppert, M. M.; van Assen, H. C.; TerHaar Romeny, B. M.; Baaijens, F. P.; Bouten, C. V. Quantification of the temporal evolution of collagen orientation in mechanically conditioned engineered cardiovascular tissues. *Ann. Biomed. Eng.* **2009**, *37*, 1263−1272.
(52) Akhyari, P.; Fedak, P. W.; Weisel, R. D.; Lee, T. Y.; Verma, S.; Mickle, D. A.; Li, R. K. Mechanical stretch regimen enhances the formation of bioengineered autologous cardiac muscle grafts. *Circulation* **2002**, *106*, I137−I142.
(53) Fink, C.; Ergun, S.; Kralisch, D.; Remmers, U.; Weil, J.; Eschenhagen, T. Chronic stretch of engineered heart tissue induces hypertrophy and functional improvement. *FASEB J.* **2000**, *14*, 669−679.
(54) Huang, G.; Pashmforoush, M.; Chung, B.; Saxon, L. A. The role of cardiac electrophysiology in myocardial regenerative stem cell therapy. *J. Cardiovasc. Trans. Res* **2011**, *4*, 61−65.
(55) Wikswo, J. P., Jr.; Lin, S. F.; Abbas, R. A. Virtual electrodes in cardiac tissue: a common mechanism for anodal and cathodal stimulation. *Biophys. J.* **1995**, *69*, 2195−2210.
(56) McDonough, P. M.; Glembotski, C. C. Induction of atrial natriuretic factor and myosin light chain-2 gene expression in cultured ventricular myocytes by electrical stimulation of contraction. *J. Biol. Chem.* **1992**, *267*, 11665−11668.
(57) Akar, F. G.; Spragg, D. D.; Tunin, R. S.; Kass, D. A.; Tomaselli, G. F. Mechanisms underlying conduction slowing and arrhythmogenesis in nonischemic dilated cardiomyopathy. *Circ. Res.* **2004**, *95*, 717−725.
(58) Kostin, S.; Dammer, S.; Hein, S.; Klovekorn, W. P.; Bauer, E. P.; Schaper, J. Connexin 43 expression and distribution in compensated and decompensated cardiac hypertrophy in patients with aortic stenosis. *Cardiovasc. Res.* **2004**, *62*, 426−436.
(59) Villa, E.; White, A. S.; Liao, J.; de Jongh Curry, A. L. An inexpensive alternative bath system for electrophysiological characterization of isolated cardiac tissue. *Conf. Proc. IEEE Eng. Med. Biol. Soc.* **2011**, *2011*, 8424−8427.
(60) Patten, R. D.; Hall-Porter, M. R. Small animal models of heart failure: development of novel therapies, past and present. *Circ.: Heart Failure* **2009**, *2*, 138−144.